JOURNAL OF Applied Polymer SCIENCE

Carbazoles on Same Main Chain for Polymer Solar Cells

Ruiping Qin, Yurong Jiang, Heng Ma, Le Yang, Hengzhi Liu, Fanggao Chang
College of Physics & Information Engineering, Key Laboratory of Photovoltaic Materials of Henan Province, Henan Normal University, Xinxiang 453007, China
Correspondence to: R. Qin (E-mail: qinruiping@163.com) or F. Chang (Email: fanggaochang@hotmail.com)

ABSTRACT: Planar conjugated 2,7-linked carbazole blocks: Q1(2,7-dibromo-9-octyl-9H-carbazole); Q2(7,7′-dibromo-9,9′-dioctyl-9H,9′H-2,2′-bicarbazole); Q3 (7-bromo-7′-(7-bromo-9-octyl-9H-carbazol-2-yl)-9,9′-dioctyl-9H,9′H-2,2′-bicarbazole) were coupled with same acceptor (4,7-di[2,5-thiophene]-5,6-dioctyloxy-2,1,3-Benzothiadiazole) to prepare polymers HXS-1, 2, 3 (Scheme 1). Bulk-heterojunction polymer solar cells (BHJ PSCs) with these polymers were made. Power conversion efficiency of HXS-1 was proved to be over 5.4%. It declined dramatically to 0.43% and 0.23% for HXS-2 and 3 respectively. Their absorption and X-ray diffraction pattern show the torsion angle in main chain increased when more carbazole units were added. More carbazoles will make polycondensation reaction more difficult to get high molecular weight polymers. The torsion angle was calculated using a semiempirical molecular orbital method. All the results pointed out that the coplanarity in the conjugated backbone was destroyed. Electron delocalization was disturbed because p-orbital overlapping only occurs effectively in the parallel orbit so charge cannot move a longer distance. This study offers a useful and important insight to designing polymers for high performance PSCs. © 2013 Wiley Periodicals, Inc. J. Appl. Polym. Sci. 129: 2671–2678, 2013

KEYWORDS: optical and photovoltaic applications; conducting polymers; morphology

Received 15 October 2012; accepted 4 January 2013; published online 30 January 2013
DOI: 10.1002/app.38996

INTRODUCTION

Much effort has been put into bulk-heterojunction (BHJ) organic photovoltaic (OPV) cells because of their potential applications.[1–3] Solution-process and effective large scale manufacture of these solar cells are promising in reducing the production cost and at the same time, meeting the clean environmental requirement for fossil fuel combustion. Although the progress in this direction is extremely encouraging and exciting, however, this art faces an obstacle of low power conversion efficiencies (PCEs) and short device lifetime.[4–6] The present state for this photovoltaic technology is that the PCE of the solar cells is just above 8%.[7–10] For commercial use PCE above 10% is desirable. To achieve high PCE, the morphology of photoactive layer is a key issue.[11–14] Ideal BHJ donor/acceptor domain length scale of $\leq$10 nm has multiple interfaces for efficient charge separation and long percolation pathways for efficient charge transfer to electrodes. Many largely experimental methods have been applied to achieve high PCE. Most concern should be the light absorption and balanced hole-electron mobility of the donor material. New conjugated polymers with proper chemical and physical properties realized impressive device efficiency.[15–18] Optical absorption must be matched with the region of maximum solar photon flux to harvest the solar energy effectively. Develop small band-gap polymers with high absorption ratio is essential to promote PCE.[19] Adjusting the band gap with deep highest occupied molecular orbital (HOMO) level while trying to keep the driving force for charge separation leads to a maximization value of V_{oc}.[20–22] From the materials Structure–Property perspective, what is the effect if the same donor blocks were repeatedly fixed to a similar main chain? The 2,7-substituted carbazole electron-donating materials have proved to be effective in improving the performance of OPV devices.[23–26] In this work, particular structure-property for a series of copolymers containing 2,7-substituted carbazoles blocks was investigated and the potential for the rational design of materials for high efficiency solar cells was discussed. 2,7-substituted polycarbazoles, with the bond angle between two 2,7-linked carbazole units closing to 180° should be ideal building blocks for rigid, rod like molecules with respect to 3,6-linked carbazole blocks.[27,28] In this article, three carbazole model building blocks (Q1, Q2, and Q3) were introduced, see Scheme 2. All these carbazole oligomers linked at 2,7 position. Their boronic esters were directly used in Suzuki–Miyaura–Schlüter reaction with 4,7-di[2,5-thiophene]-5,6-dioctyloxy-

Additional Supporting Information may be found in the online version of this article.

Applied Polymer SCIENCE

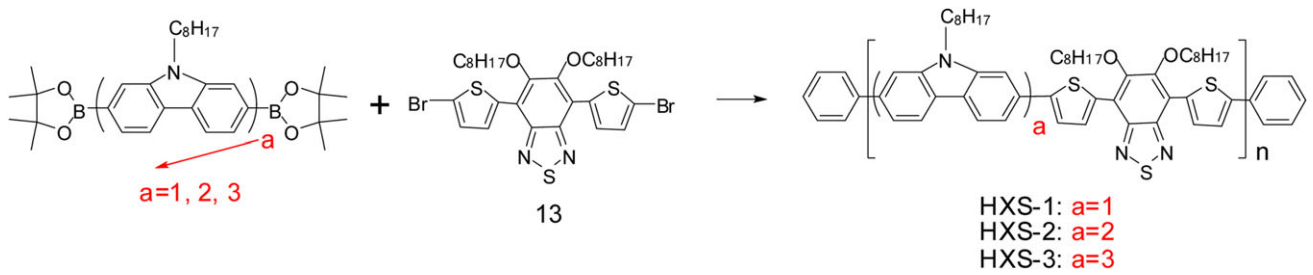

Scheme 1. Synthesis of polymers HXS-1, 2, 3. [Color figure can be viewed in the online issue, which is available at wileyonlinelibrary.com.]

2,1,3-Benzothiadiazole to prepare polymers HXS-2 and HXS-3, see Scheme 1. The preparing procedure for HXS-1 can be find in Ref. [29]. This work provides an insight into the structure–property designing for high performance polymer solar cells (PSCs).

EXPERIMENTAL

Materials

All chemicals were bought from Aldrich or Acros and used without further purification. The catalyst precursor, $Pd(PPh_3)_4$, was prepared according to the literature.[30] The solvents were dried according to standard procedures. All reactions were performed under an atmosphere of nitrogen and monitored by thin-layer chromatography with silica gel (GF254). Column chromatography was carried out on silica gel (200–300 mesh).

Characterization

^{1}H- and ^{13}C-NMR was recorded on a Bruker AV400 spectrometer in $CDCl_3$. Electronic absorption were obtained on a Shimadzu model UV-3600 PC ultraviolet–visible (UV–vis) spectrometer. Elemental analyses were performed on a Flash EA 1112 analyzer. Powder X-ray diffraction (XRD) patterns were obtained by Cu KR radiation on a PANalytical X′ Pert PROMPD diffract meter. The electrochemical behavior of HXS-1,2,3 were investigated by cyclic voltammeter (CHI 630A Electrochemical Analyzer) use a standard three-electrode electrochemical cell, in a 0.1*M* tetrabutylammonium tetrafluoro borate solution in CH_3CN , at room temperature and at N_2 atmosphere with a scanning rate of 0.1 V/s^{-1}. A glassy carbon working electrode, a Pt wire counter electrode, and an $Ag/AgNO_3$ (0.01*M* in CH_3CN) reference electrode were used. The experiments were calibrated with the standard ferrocene/ferrocenium (Fc) redox system, assuming that the energy level of Fc is 4.8 eV below vacuum.[31] The thermal gravimetric analysis (TGA) was carried out under a nitrogen atmosphere using a Pyris-1 TGA instrument with a heating rate of 10°C/min to record trace. Gel permeation chromatography (GPC) measurements

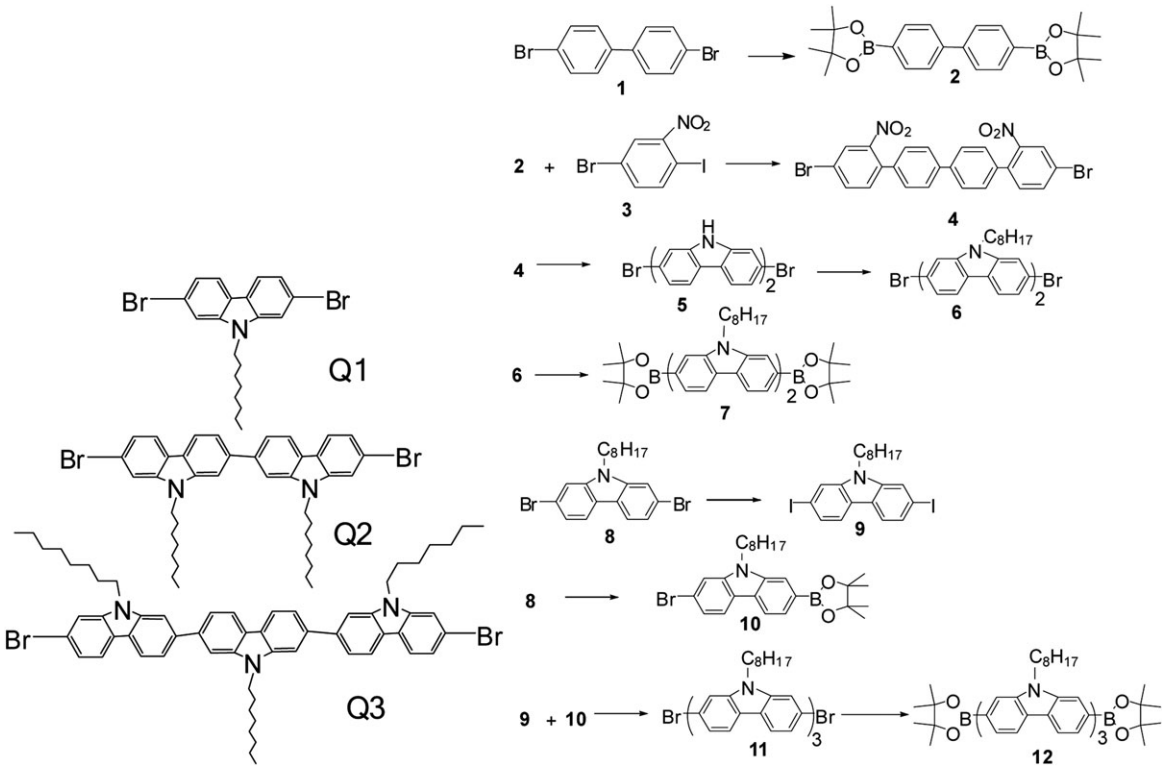

Scheme 2. The chemical structure of Q1, Q2, Q3, and Synthesis of monomers 1–12.

were performed on a Waters chromatography connected to a Water 410 differential refract meter with chloroform as an eluent. Atomic force microscopy (AFM) measurements were performed under ambient conditions using a Digital Instrument Multimode Nanoscope IIIA operating in the tapping mode. Organic solar cells (OSCs) were fabricated with the device configuration of ITO/PEDOT : PSS/active layer/LiF/Al. The conductivity of ITO was 20 Ω/□ and PEDOT : PSS is Baytron AI 4083 from H. C. Starck. A thin layer of PEDOT : PSS was spin coated on top of cleaned ITO substrate at 2500 rpm/s and dried subsequently at 120°C for 10 min on a hotplate before being transferred into a glove box. The active layer was prepared by spin-coating dichlorobenzene solution of polymers and $PC_{71}BM$ on the top of ITO/PEDOT : PSS. The top electrode was thermally evaporated, with a 0.6 nm LiF layer, followed by 80 nm of aluminum at a pressure of 10^{-6} Torr through a shadow mask. Four OSCs were fabricated on one substrate and the effective area of one cell is roughly 4 mm^2. Current-voltage characteristics were recorded using a Keithley 2400 Source Meter under AM 1.5 illumination with an intensity of 100 mW/cm^2 from a solar simulator (Model SS-50A, photo Emission Tech).

Synthesis

General procedures for preparing polymers HXS-2, 3 were similar to that for HXS-1. See Scheme 1.

A mixture of monomers, THF or THF/Toluene, water, $NaHCO_3$ and the catalyst forerunner $Pd(PPh_3)_4$ was carefully degassed and charged with nitrogen. The reaction mixture was stirred and refluxed for 3 days. Phenyl boronic acid and bromobenzene were used consecutively to end-cap the polymer after polymerization. $CHCl_3$ was then added; the organic layer was separated and dried over Na_2SO_4. After the removal of most solvent, the residue was collected by filtration. The crude product was dissolved in a minimum amount of $CHCl_3$, and precipitated into a large amount of acetone. The formed dark precipitates were collected by filtration and dried in high vacuum.

HXS-2. Compound 7 (0.20 g, 0.25 mmol), 13 (0.18 g, 0.25 mmol), THF (30 mL), Toluene (10 mL), H_2O (6 mL), $NaHCO_3$ (1.2 g, 14.4 mmol), and $Pd(PPh_3)_4$ (1.8 mg, 1.6 μmol) were used. 250 mg (a yield of 90%) of HXS-2 was obtained. ^{1}H-NMR (400 MHz, $CDCl_3$ δ:) 8.59–7.51 (broad, 16H), 4.51–4.44 (t, 4H), 4.27–4.25 (t, 4H), 2.08–2.02 (m, 8H), 1.59–1.29 (broad, 40H), 0.91–0.87 (broad, 12H). ^{13}C-NMR (100 MHz, $CDCl_3$ δ:) 190.90, 176.52, 131.07, 128.79, 127.45, 31.91, 31.87, 29.75, 29.46, 29.27, 27.45, 24.15, 22.73, 22.64, 14.12, and 14.08.

HXS-3. Compound 12 (0.20 g, 0.18 mmol), 13 (0.13 g, 0.18 mmol), THF (30 mL), Toluene (10 mL), H_2O (6 mL), $NaHCO_3$ (1.2 g, 14.4 mmol) and $Pd(PPh_3)_4$ (1.8 mg, 1.6 μmol) were used. 200 mg (a yield of 78%) of HXS-3 was obtained. ^{1}H-NMR (400 MHz, $CDCl_3$ δ:) 8.60–7.43 (m, 22H), 4.49–4.42 (broad, 4H), 4.23–4.17 (m, 6H), 2.06–1.99 (m, 10H), 1.35–1.30 (broad, 50H), 0.94–0.92 (broad, 15H). ^{13}C-NMR (100 MHz, $CDCl_3$ δ:) 151.68, 150.93, 141.72, 141.44, 140.27, 133.32, 132.03, 123.04, 122.41, 121.88, 120.55, 119.22, 117.47,107.69, 74.50, 43.14, 31.91, 31.86, 30.64, 29.74, 29.47, 29.43, 29.27, 29.11, 27.44, 26.20, 22.72, 22.64, 14.13, and 14.09.

Preparation of Monomers. See Scheme 2.

4,4′-bis(4,4,5,5-tetramethyl-1,3,2-dioxaborolan-2-yl)biphenyl (2). compound 1 (5.0 g, 16 mmol); 4,4,4′,4′,5,5,5′,5′-octamethyl-2,2′-bi(1,3,2-dioxaborolane) (10.2 g, 40 mmol); potassium acetate (4.4 g, 45 mmol), $Pd(dppf)_2CL_2$(150 mg) were dissolved in 80 mL DMF. The mixture was reacted for 48 h at 80°C. Then 250 mL H_2O was added .The organics were extracted with diethyl ether (3 × 50 mL). The combined organics were dried over anhydrous Na_2SO_4 and filtered. Removal of the solvent on a rotary evaporator gave black oil. The crude product was then purified by column chromatography on silica gel (hexane/ethyl acetate; 15/1) to give 5.0 g (76.8%, yield) white powder of title compound 2. ^{1}H: NMR (400 MHz, $CDCl_3$): δ 7.89–7.87 (d, 4H), 7.64–7.62 (t, 4H), 1.365 (s, 24H).

Compound (4). A mixture of compound 2 (2.5 g, 6.16 mmol) and 4-bromo-1-iodo-2-nitrobenzene 3 (4.5 g, 13.5 mmol), K_2CO_3 (2.0 g, 14.5 mmol), THF (50. mL), toluene (50. mL) water (10 mL) was carefully degassed and charged with nitrogen before and after $Pd(PPh_3)_4$ (200 mg) was added. The mixture was heated to 50°C and stirred for 1 day, and then the reaction temperature was increased to 80°C and the reaction mixture was further stirred for another day. After it was cooled to room temperature, the mixture was poured and stirred into 200 mL methanol, the resulted precipitate was collected by filtration. The crude products were washed with water (200 mL) and then methanol (50 mL). 3.4 g yellow powder was obtained. The compound 4 goes to next step without further purification.

7,7′-dibromo-9H,9′H-2,2′-bicarbazole (5). A mixture of compound 4 (3 g, 5.4 mmol) and 15 mL of triethyl phosphate was heated under reflux for 24 h. Methanol (100 mL) was added and the resulted precipitate was collected by filtration. The crude products were washed with water (100 mL) and then methanol (50 mL). 1.68 g white powder was obtained. The compound 5 goes to next step without further purification.

7,7′-dibromo-9,9′-dioctyl-9H,9′H-2,2′-bicarbazole (6). Sodium hydride (NaH) (1.68 g, 65 mmol) was added to a solution of 5 (1.68 g, 3.06 mmol) in 80 mL of DMF. The solution was stirred at room temperature for 0.5 h, and then 1-brome-octane (3g, 11.8 mmol) was drop vise added. The mixture was stirred at room temperature for 24 h and then quenched with 50 mL water. The aqueous layer was extracted with dichloromethane (3 × 30 mL). The organic layer was dried over anhydrous Na_2SO_4 and the solvent was removed under reduced pressure. The residue was purified by column chromatography on silica gel, (dichloromethane/hexane, 1 : 10) to provide 1.42 g of the title compound as a white powder (Yield: three steps total 40%).

Table I. Number Average Molecular Weight (M_n), Weight Average Molecular Weight (M_w), PDI, Degradation Temperature (T_d), and Glass Transition Temperatures (T_g) of HXS-1, 2, 3

Polymers	M_n	M_w	PDI	T_d(°C)	T_g(°C)
HXS-1	16,600	51,400	3.10	300.5	105.0
HXS-2	6270	11,600	1.84	317.5	58.9
HXS-3	1170	2000	1.75	312.3	96.9

^{1}H-NMR ($CDCl_3$, 400 MHz δ:): 8.16–8.14 (d, 2H), 7.99–7.97(d, 2H), 7.67(s, 2H), 7.62–7.59(m, 4H), 7.39–7.36(d, 2H), 4.35–4.32(t, 4H), 1.95–1.91(t, 4H), 1.44–1.27(m, 20H), 0.89–0.86(t, 6H). ^{13}C-NMR (100 MHz, $CDCl_3$ δ:) 141.77, 141.14, 140.49, 122.11, 121.60, 121.52, 121.48, 120.57, 119.57, 111.81, 107.89, 43.25, 31.79, 29.36, 29.19, 28.92, 27.29, 22.60, and 14.06.

9,9′-dioctyl-7,7′-bis(4,4,5,5-tetramethyl-1,3,2-dioxaborolan-2-yl)-9H,9′H-2,2′-bicarbazole (7). 6 (1.0 g, 1.4mmol), 4,4,4′,4′,5,5,5′,5′-octamethyl-2,2′-bi(1,3,2-dioxaborolane) (1.0 g, 4.2 mmol), potassium acetate (0.44 g, 0.45 mmol), $Pd(dppf)_2CL_2$(50 mg.) was dissolved in 30 mL DMSO. The mixture was reacted for 48 h at 80°C. Then, 150 mL H_2O was added. The organics were extracted with diethyl ether (3 × 20 mL). The combined organics were dried over anhydrous Na_2SO_4 and filtered. Removal of the solvent on a rotary evaporator gave black oil. The crude product was then purified by column chromatography on silica gel (hexane/ethyl acetate; 15/1) to give 0.85 g light yellow powder (65%, yield).

^{1}H: NMR (400 MHz, $CDCl_3$ δ:) 8.23–8.21 (d, 2H), 8.16–8.14 (d, 2H), 7.92 (s, 2H), 7.74–7.71 (m, 4H),7.62–7.60 (d, 2H),4.46–4.42 (t, 4H), 1.97–1.94 (t, 4H), 1.43–1.26 (m, 44H), 0.87–0.86 (t, 6H). ^{13}C-NMR (100 MHz, $CDCl_3$ δ:) 140.81, 140.48, 125.20, 125.13, 121.77, 120.94, 119.60, 119.06, 115.04,107.88,107.03, 83.76, 31.81, 29.39, 29.20, 29.12, 27.27, 24.94, 22.60, and 14.05.

RESULTS AND DISCUSSION

Synthesis

The synthesis of these 2,7-linked carbazole oligomers was illustrated in Scheme 2. Q1 was synthesized according to published literature[32]; Synthesis of Q2 began by transfering 4,4′-dibromobiphenyl to boronic ester compound 2 in a 76.8% yield. Compound 2 was then coupled to 4-bromo-1-iodo-2-nitrobenzene monomer 3 by Suzuki–Miyaura cross-coupling reaction to obtain four quantificational. Monomer 5 was obtained through the Cadogan reaction in a proper yield. Three steps from compound 2 to compound 6 (Q2) in a total 41% yield was realized. For the synthesis of Q3 see our published work.[33] These 2,7-linked carbazole blocks (Q1, Q2, and Q3) were coupled with same blocks (4,7-di[2,5-thiophene]-5,6-dioctyloxy-2,1,3-Benzothiadiazole) to get three polymers HXS-1, 2, 3.

HXS-1 has been reported in our previous work.[29] HXS-2, 3 were synthesized with the same procedure. The structures of these polymers were confirmed by ^{1}H- and ^{13}C-NMR spectroscopy. Molecular weights of these polymers were measured by GPC calibrated with polystyrene standards at 150°C with 1,2,4-trichlorobenzene as an eluent for HXS-1, and chloroform as an eluent for HXS-2 and HXS-3 at room temperature. The data were summarized in Table I. Considerably high molecular weights have been achieved for HXS-1 so that it was only soluble in warm solvent.

The relatively low molecular weight for polymer HXS-2 and HXS-3 was probably due to their poor solubility in the organic solvents used in the polycondensation. They precipitated from the reaction media during the polycondensation. Especially for HXS-3, the GPC indicates that only one coupling between a donor and an acceptor unit has taken place. Fortunately, the precipitated polymers are readily soluble in chloroform and 1,2-dichlorobenzene (DCB). Thermo gravimetric analysis (TGA) indicated that all polymers have good thermal stability. Glass transition temperatures (T_g) of the three polymers are also listed in Table I, among which HXS-2 shows relatively lower T_g of 58.9°C. That maybe due to the larger torsion angle which caused poor crystalline (Figure 3).

Optical Properties and Torsion Angle

UV–vis absorption of samples Q1, Q2, and Q3 in dilute THF solutions were shown in Figure 1. All the carbazole oligomers presented a broad absorption ranging from 210 to 425 nm. With increasing the conjugation oligomers, the onset of the absorption spectra red shifts from 358 nm for Q1 to 387 nm for Q2, and 400 nm for Q3. The absorption spectra demonstrate that these monomers can broaden polymer absorbance spectra when they were polycondensed with other building blocks to make conjugated semiconductive polymers. The absorption spectra are very important for PSCs or organic light-emitting diode. Their ^{1}H-NMR spectra show nice and clean chemistry. However, when these monomers copolymerized with the same electron-deficient block to make polymers HXS-1, 2, 3, the polymers absorption spectra show a blue shift as the number of the carbazole units increases, either in solutions B or in films C (Figure 1). The absorption bands of these three polymers all red-shift and become broader when they go from the solutions to the solid states. An absorption peak appears at 564,

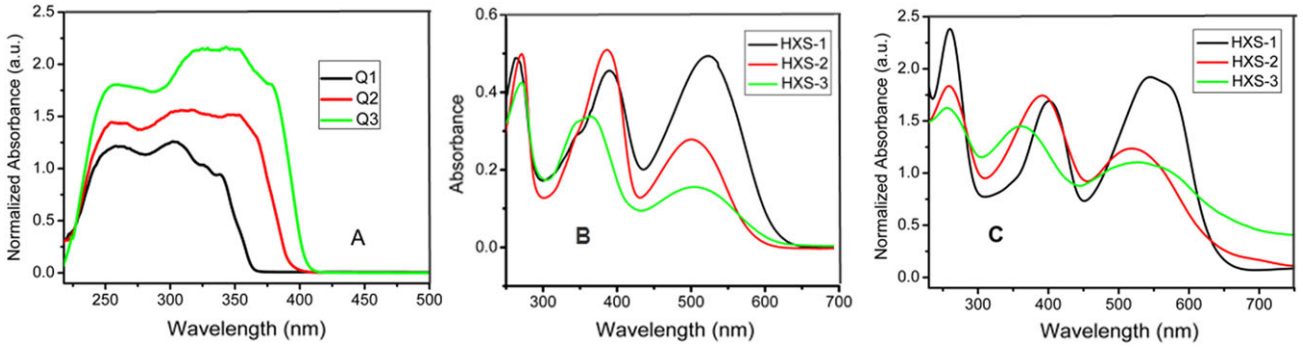

Figure 1. UV–vis absorption spectra of Q1, Q2, and Q3 in THF A and their corresponding polymers HXS-1, 2, 3 spectra in $CHCl_3$ (concentration: 8.4 × 10^{-3} mg/mL) B and in films C. [Color figure can be viewed in the online issue, which is available at wileyonlinelibrary.com.]

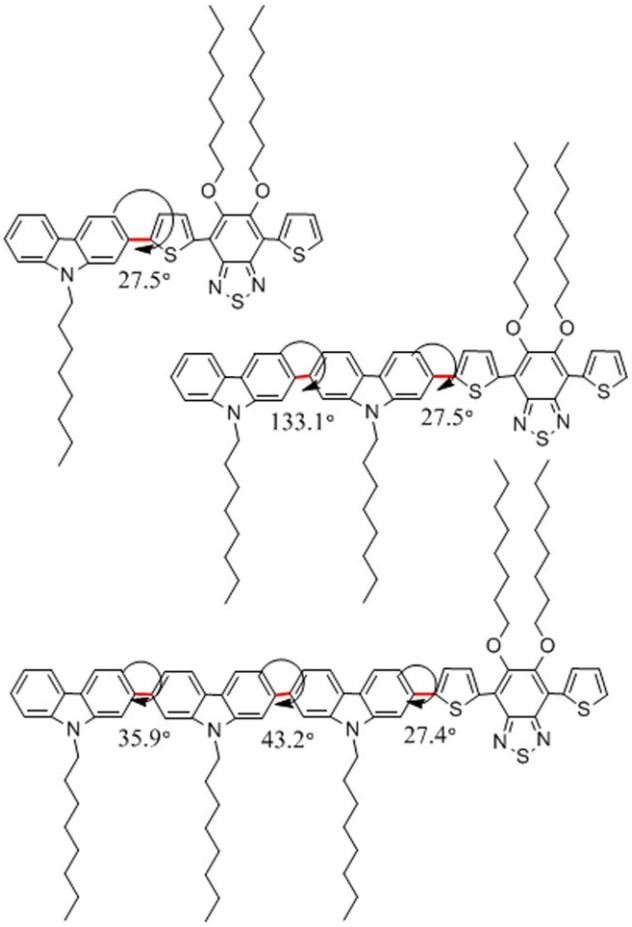

Figure 2. The torsion angle between different planar blocks. [Color figure can be viewed in the online issue, which is available at wileyonline library.com]

527, and 535 nm and a second peak at 403, 396, and 363 nm for HXS-1, HXS-2, and HXS-3 films, respectively. The red shift that occurs during the transformation from the solution to the film state is attributed to the aggregation of the polymer chains or the orderly π–π stacking formed in the solid states. The

Table II. Characteristic Properties of Polymers/$PC_{71}BM$ Solar Cells

Active layer	Thickness (nm)	J_{sc} (mA/cm^2)	V_{oc} (V)	FF	PCE (%)
HXS-1/$PC_{71}BM$	100	10.04	0.85	0.65	6.21
HXS-2/$PC_{71}BM$	108	2.79	0.75	0.21	0.43
HXS-3/$PC_{71}BM$	95	1.93	0.54	0.23	0.23

absorption red-shifts for HXS-1, HXS-2, and HXS-3 are 33, 24, and 28 nm, respectively. Smaller red-shift for HXS-2 and HXS-3 can be attributed to the replacement of one carbazole unit by two or three to increase the twist of the polymer backbone and decrease the aggregation effect in solid state. It is obvious that the increase of the carbazole units in HXS-2 and HXS-3 lowers the light absorption ability at a wavelength range from 420 to 650 nm which is also an important part of solar spectrum for solar cells. This also explained the PCE decline for devices made from polymers HXS-2, 3.

For the torsion angle between different planar blocks, a computer simulation was carried out for these molecules. In our calculation, the energy-minimization and structural-optimization have been determined using a semiempirical molecular orbital package (MOPAC2000) with the key words AM1 and POLAR. The calculated result shows almost equal torsion angles between the first carbazole and benzothiadiazole (Figure 2). The torsion angle between the planar carbazole and carbazole in HXS-2 is 133.1°. This angle is 35.9° at the second and third carbazole unit in HXS-3. The large torsion angle breaks the conjugated backbone sharply and results in a blue shift of the absorption spectra. For PSCs, mismatch of the absorption spectra with the solar spectrum will decline the PCE fiercely. The information on torsion angle should be very useful for people specialized in this research field.

Photovoltaic Properties and Device Morphology

Additives have notable influence on the photovoltaic performance. 1,8-Diiodooctane (DIO) was chosen to optimize the morphology in all device building. The photovoltaic features of

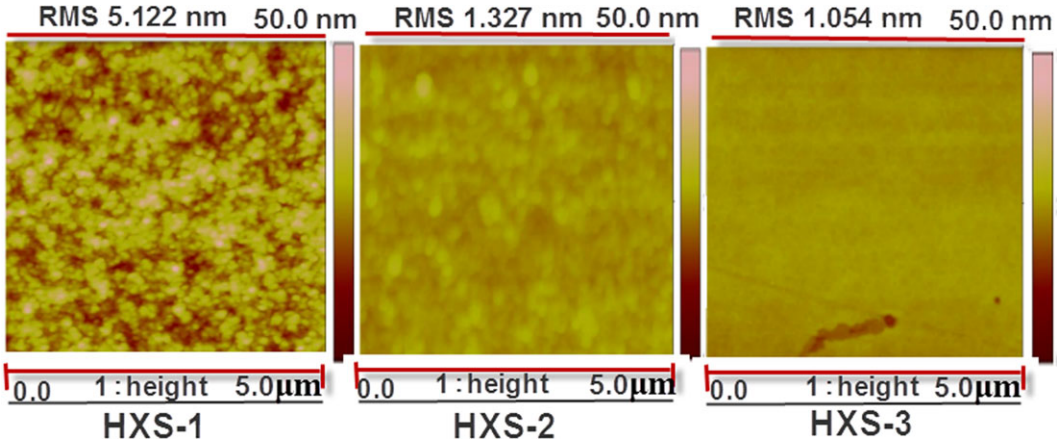

Figure 3. AFM images (5 × 5 μm^2) of the active layers from the blend of the polymer and $PC_{71}BM$ (polymer: $PC_{71}BM$ = 1 : 3). With DIO (v/v = 2.5%). [Color figure can be viewed in the online issue, which is available at wileyonlinelibrary.com.]

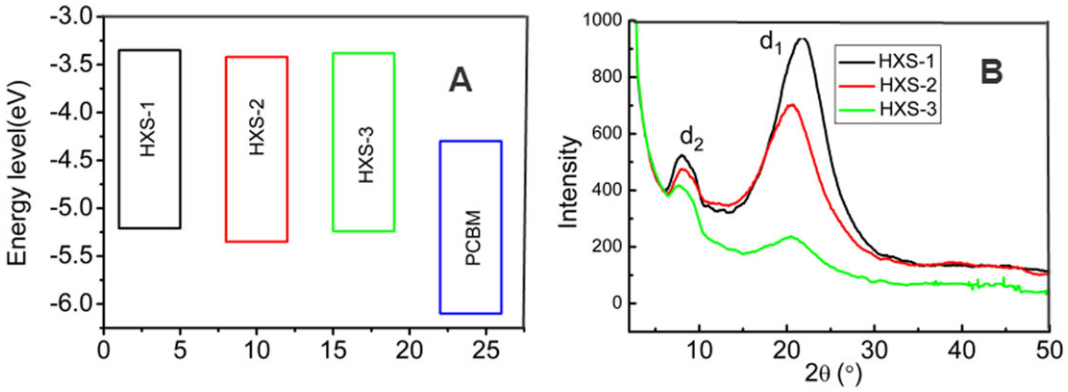

Figure 4. Energy level diagrams (A) and XRD patterns of powdery HXS-1, 2, 3 (B). [Color figure can be viewed in the online issue, which is available at wileyonlinelibrary.com.]

solar cells are shown in Table II. The device made from the blend of each polymer and $PC_{71}BM$ in DCB solution show different photovoltaic performance. For HXS-1, we previously reported a PCE of 5.4%. After further optimizing (adjust the real cell area), the highest PCE up to 6.34% was reached with a V_{oc} of 0.85 V, J_{sc} of 10.47 mA/cm^2 and FF of 0.63. A mean PCE of 6.21% with a V_{oc} of 0.85 V, J_{sc} of 10.04 mA/cm^2 and FF of 0.65 was obtained by averaging over six solar cells. The PCE for HXS-2 decreased to 0.43% with V_{oc} of 0.75 V, J_{sc} of 2.79 mA/cm^2 and FF of 0.21. For HXS-3, the PCE further decreased to 0.23% with V_{oc} of 0.54 V, J_{sc} of 1.93 mA/cm^2 and FF of 0.23. Both devices based on HXS-2 and HXS-3 display declined PCEs. This is ascribed to the decreased J_{sc} and FF due to the lower molecular weight and bad morphology of the specimen. The morphology of the blend films spin-coated from the polymers and $PC_{71}BM$ in DCB solution with DIO was examined by tapping-mode AFM. Height images of spin-coated blend films are shown in (Figure 3), together with the root-mean-square (RMS) values are also summarized on these images. DIO has a higher boiling point than the host solvent, PCBM tends to remain in solution (during drying) longer than the blend polymer, since the fullerenes was selectively dissolved in DIO, which can be used to control the phase separation and the resulting morphology of the BHJ material. As shown in Figure 3, HXS-1 blend films show perfect morphology with RMS 5.122 nm. From HXS-1 to HXS-2 and then HXS-3 the surface of blend films becomes smoother. RMS decreased to 1.327 nm and 1.054 nm. No large domains could be observed in HXS-3, suggesting no obvious phase separations occur. It is well-known that a certain degree of phase separation is necessary to provide a percolation pathway for charge transportation to the electrodes. Lack of phase separation maybe the main reason for the bad device performance. We also measured the external quantum efficiency (EQE) To confirm the accuracy of the J_{sc} conducted on the devices under illumination of monochromatic light. As shown in [Figure 5(B)], the solar cells show a lower EQE values not more than 30% for HXS-2 and an even smaller EQE values below 5% for HXS-3. Maximum EQE of ~70% for HXS-1 which is consistent with the PCE [Figure 5(A)]. The J_{sc} calculated from integration of the EQE with an AM 1.5G reference spectrum agreed well with the J_{sc} obtained from the J–V measurements.

Energy Level and Crystalline

Three polymers have similar energy level [Figure 4(A)]. The lowest unoccupied molecular orbital (LUMO) and HOMO energy levels were determined by a cyclic voltammogram to be −3.35 and −5.21 eV for HXS-1; −3.39 and −5.35 eV for HXS-

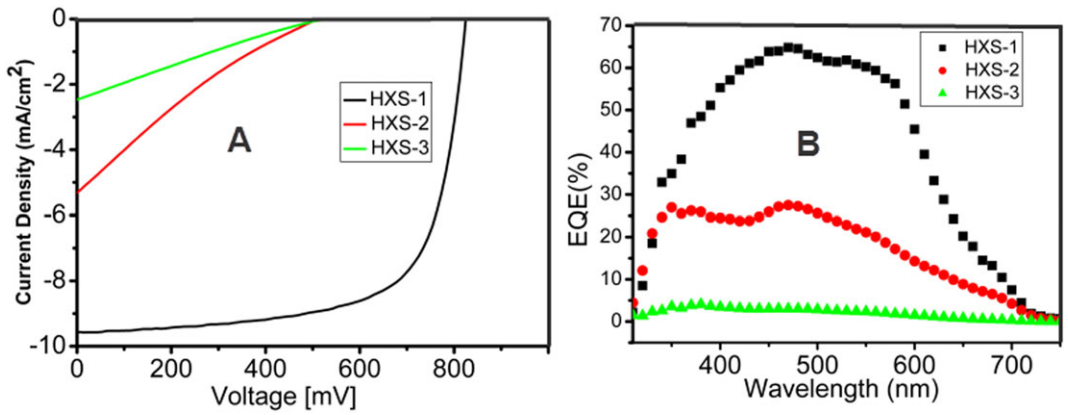

Figure 5. (A) *I–V* curves and (B) EQEs for solar cells based on HXS-1, 2, 3/$PC_{71}BM$ processed with 2.5% (v/v) DIO in DCB. [Color figure can be viewed in the online issue, which is available at wileyonlinelibrary.com.]

2; −3.34 and −5.24 eV for HXS-3, respectively. The band gap (Eg) was determined from the onset of the absorption to be 1.95 eV for HXS-1, 1.96 eV for HXS-2 and 1.90 eV for HXS-3. The XRD pattern of three powdery polymers shows two peaks: the first peak at 7.96° for HXS-1, 8.12° for HXS-2, and 7.87° for HXS-3 reveals that the distance between polymer main chains separated by equal number of carbon alkyl side chains is almost the same value ~11 Å; the second peak at 22.01° for HXS-1, 20.59° for HXS-2, and 20.34° for HXS-3 reveals that a π–π distance of ~4.03 Å between polymer main chains of HXS-1 increases to ~4.31 Å for HXS-2, and further to ~4.36 Å for HXS-3. This suggests that the polymer planar conformation chain is twisted and broken in solid state [Figure 4(B)]. The large intermolecular distance results in poor morphology of the blend film (Figure 3).

CONCLUSIONS

In summary, mono dispersed 2,7-linked carbazole functional building blocks was synthesized by modular chemistry. The absorption spectra for 2,7-linked carbazole building blocks are in the ultraviolet region. The absorption spectra become broaden and red-shifted when more carbazole is linked. These carbazole monomers can reduce the polymer's band-gap to obtain more solar energy which is important in polymeric photovoltaic solar cells. However, our work shows just the opposite when they are copolymerized with an identical monomer. More carbazole will lower the molecular weight and increase the torsion angle, leading to a dramatic decline in the PCE. The torsion angles between different monomers play an important role in high performance polymers used for PSCs.

ACKNOWLEDGMENTS

The authors thank the financial support by the Postdoctoral Starting Foundation of Henan Normal University (01026500105) and Young Scientists Foundation of Henan Normal University (01026400061).

REFERENCES

1. Qin, R.-P.; Song, G.-L.; Jiang, Y.-R.; Bo, Z.-S. *Chem. J. Chin Univ (Chinese)* **2012**, *33*, 828.
2. Piliego, C.; Holcombe, T. W.; Douglas, J. D.; Woo, C. H.; Beaujuge, P. M.; Frechet, J. M. J. *J. Am. Chem. Soc.* **2010**, *132*, 7595.
3. Brabec, C. J.; Dyakonov, V.; Scherf, U. Organic Photovoltaics: Materials, Device Physics, and Manufacturing Technologies, **2008**; Vol. 1, Chapter 1, pp 3–5.
4. Aguirre, A.; Meskers, S. C. J.; Janssen, R. A. J.; Egelhaaf, H. *J. Org. Electron.* **2011**, *12*, 1657.
5. Gevorgyan, S. A.; Medford, A. J.; Bundgaard, E.; Sapkota, S. B.; Schleiermacher, H.-F.; Zimmermann, B.; Würfel, U.; Chafiq, A.; Lira-Cantu, M.; Swonke, T.; Wagner, M.; Brabec, C. J.; Haillant, O.; Voroshazi, E.; Aernouts, T.; Steim, R.; Hauch, J. A.; Elschner, A.; Pannone, M.; Xiao, M.; Langzettel, A.; Laird, D.; Lloyd, M. T.; Rath, T.; Maier, E.; Trimmel, G.; Hermenau, M.; Menke, T.; Leo, K.; Rösch, R.; Seeland, M.; Hoppe, H.; Nagle, T. J.; Burke, K. B.; Fell, C. J.; Vak, D.; Singh, T. B.; Watkins, S. E.; Galagan, Y.; Manor, A.; Katz, E. A.; Kim, T.; Kim, K.; Sommeling, P. M.; Verhees, W. J. H.; Veenstra, S. C.; Riede, M.; Greyson Christoforo, M.; Currier, T.; Shrotriya, V.; Schwartz, G.; Krebs, F. C. *Solar Energy Mater. Solar Cells* **2011**, *95*, 1398.
6. Reese, M. O.; Gevorgyan, S. A.; Jørgensen, M.; Bundgaard, E.; Kurtz, S. R.; Ginley, D. S.; Olson, D. C.; Lloyd, M. T.; Morvillo, P.; Katz, E. A.; Elschner, A.; Haillant, O.; Currier, T. R.; Shrotriya, V.; Hermenau, M.; Riede, M.; R. Kirov, K.; Trimmel, G.; Rath, T.; Inganäs, O.; Zhang, F.; Andersson, M.; Tvingstedt, K.; Lira-Cantu, M.; Laird, D.; McGuiness, C.; Gowrisanker, S.; Pannone, M.; Xiao, M.; Hauch, J.; Steim, R.; DeLongchamp, D. M.; Rösch, R.; Hoppe, H.; Espinosa, N.; Urbina, A.; Yaman-Uzunoglu, G.; Bonekamp, J.-B.; van Breemen, A. J. J. M.; Girotto, C.; Voroshazi, E.; Krebs, F. C. *Solar Energy Mater. Solar Cells* **2011**, *95*, 1253.
7. Liang, Y.; Xu, Z.; Xia, J.; Tsai, S.-T.; Wu, Y.; Li, G.; Ray, C.; Yu, L. *Adv Mater.* **2010**, *22*, E135.
8. Liang, Y.; Yu, L. *Acc. Chem. Res.* **2010**, *43*, 1227.
9. Price, S. C.; Stuart, A. C.; Yang, L.; Zhou, H.; You, W. *J. Am. Chem. Soc.* **2011**, *133*, 4625.
10. Li, W.; Roelofs, W. S. C.; Wienk, M. M.; Janssen, R. A. J. *J. Am. Chem. Soc.* **2012**, *134*, 13787.
11. Fan, H.; Zhang, M.; Guo, X.; Li, Y.; Zhan, X. *ACS Appl. Mater. Interfaces* **2011**, *3*, 3646.
12. Li, W.; Zhou, Y.; Viktor Andersson, B.; Mattias Andersson, L.; Thomann, Y.; Veit, C.; Tvingstedt, K.; Qin, R.; Bo, Z.; Inganäs, O.; Würfel, U.; Zhang, F. *Org. Electron.* **2011**, *12*, 1544.
13. Shi, Q.; Fan, H.; Liu, Y.; Chen, J.; Ma, L.; Hu, W.; Shuai, Z.; Li, Y.; Zhan, X. *Macromolecules* **2011**, *44*, 4230.
14. Shi, Q.; Fan, H.; Liu, Y.; Hu, W.; Li, Y.; Zhan, X. *Macromolecules* **2011**, *44*, 9173.
15. He, Z.; Zhong, C.; Huang, X.; Wong, W.-Y.; Wu, H.; Chen, L.; Su, S.; Cao, Y. *Adv. Mater.* **2011**, *23*, 4636.
16. Seo, J. H.; Gutacker, A.; Sun, Y.; Wu, H.; Huang, F.; Cao, Y.; Scherf, U.; Heeger, A. J.; Bazan, G. C. *J. Am. Chem. Soc.* **2011**, *133*, 8416.
17. Wang, M.; Hu, X.; Liu, P.; Li, W.; Gong, X.; Huang, F.; Cao, Y. *J. Am. Chem. Soc.* **2011**, *133*, 9638.
18. Wang, E.; Ma, Z.; Zhang, Z.; Vandewal, K.; Henriksson, P.; Inganäs, O.; Zhang, F.; Andersson, M. R. *J. Am. Chem. Soc.* **2011**, *133*, 14244.
19. Armstrong, N. R.; Veneman, P. A.; Ratcliff, E.; Placencia, D.; Brumbach, M. *Acc. Chem. Res.* **2009**, *42*, 1748.
20. Ding, P.; Chu, C.-C.; Zou, Y.; Xiao, D.; Pan, C.; Hsu, C.-S. *J. Appl. Polym. Sci.* **2012**, *123*, 99.
21. He, Y.; Chen, H.-Y.; Hou, J.; Li, Y. *J. Am. Chem. Soc.* **2010**, *132*, 1377.
22. Cheng, Y.-J.; Hsieh, C.-H.; He, Y.; Hsu, C.-S.; Li, Y. *J. Am. Chem. Soc.* **2010**, *132*, 17381.
23. Li, J.; Grimsdale, A. C. *Chem. Soc. Rev.* **2010**, *39*, 2399.
24. Park, S. H.; Roy, A.; Beaupre, S.; Cho, S.; Coates, N.; Moon, J. S.; Moses, D.; Leclerc, M.; Lee, K.; Heeger, A. *J. Nat. Photon.* **2009**, *3*, 297.

25. Blouin, N.; Michaud, A.; Leclerc, M. *Adv. Mater.* **2007**, *19*, 2295.

26. Blouin, N.; Leclerc, M. *Acc. Chem. Res.* **2008**, *41*, 1110.

27. Kim, H. U.; Mi, D.; Kim, J.-H.; Park, J. B.; Yoon, S. C.; Yoon, U. C.; Hwang, D.-H. *Solar Energy Mater. Solar Cells* **2012**, *105*, 6.

28. Romero, D. B.; Schaer, M.; Leclerc, M.; Adês, D.; Siove, A.; Zuppiroli, L. *Synth. Met.* **1996**, *80*, 271.

29. Qin, R.; Li, W.; Li, C.; Du, C.; Veit, C.; Schleiermacher, H.-F.; Andersson, M.; Bo, Z.; Liu, Z.; Inganäs, O.; Wuerfel, U.; Zhang, F. *J. Am. Chem. Soc.* **2009**, *131*, 14612.

30. Tolman, C. A.; Seidel, W. C.; Gerlach, D. H. *J. Am. Chem. Soc.* **1972**, *94*, 2669.

31. Pommerehne, J.; Vestweber, H.; Guss, W.; Mahrt, R. F.; Bässler, H.; Porsch, M.; Daub, J. *Adv. Mater.* **1995**, *7*, 551.

32. Fu, Y.; Bo, Z. *Macromol. Rapid Commun.* **2005**, *26*, 1704.

33. Qin, R.; Bo, Z. *Macromol. Rapid Commun.* **2012**, *33*, 87.